

Time resolution at the quantum limit of two incoherent sources based on frequency resolved two-photon-interference

Salvatore Muratore^{1, 2} and Vincenzo Tamma^{1, 3, 2, *}

¹*School of Mathematics and Physics, University of Portsmouth, Portsmouth PO1 3QL, UK*

²*Quantum Science and Technology Hub, University of Portsmouth, Portsmouth PO1 3QL, UK*

³*Institute of Cosmology and Gravitation, University of Portsmouth, Portsmouth PO1 3FX, UK*

(Dated: February 10, 2026)

The Rayleigh criterion is a widely known limit in the resolution of incoherent sources with classical measurements in the spatial domain. Unsurprisingly the estimation of the time delay between two weak incoherent signals is afflicted by an analogue problem. In this work, we show the emergence of two-photon quantum beats in the frequency domain from the interference at a beam splitter of a photon emitted by a reference source and one from the two incoherent weak signals. We demonstrate, based on this phenomena, that with a relatively low number of measurements of the frequencies of the interfering photons either bunching or antibunching at the beam splitter output one can achieve a precision amounting to half of the quantum limit, independently of both the temporal shape of the photonic wavepacket and the time delay to be estimated. The feasibility of the technique makes it applicable in astronomy, microscopy, remote clocks synchronization and radar ranging.

Introduction The estimation of the time delay between two signals has a wide spectrum of applications, such as medical imaging [1], distance estimation by time of flight measurements [2], gravitational waves detection [3]. However, in those scenarios in which the signals emitted from the sources could be purely incoherent commonly employed direct time resolved detection methods drastically fail, as they are indeed unable to precisely estimate the time delay between the two signals when it becomes much smaller than the temporal width of the optical field [4], a situation analogous to the one in the spatial domain due to the Rayleigh's limit [5]. Nevertheless, thanks to the tools of quantum metrology [6], it has been shown that this is not a fundamental limit but instead a limitation of the current methods [7], and that the highest resolution achievable is the same at all scales, meaning that it is possible in theory to devise a high precision sensing scheme free from such limit. As a consequence, the research for a solution has led to the development of new approaches, among which the state-of-art is represented by temporal modes decomposition methods [7–9]. This technique relies on a mode selective projection of the wavepacket of the incoming photons into orthogonal temporal modes, performed by mixing the incoming signals with specifically constructed gating pulses through a properly engineered waveguide, after which photon counting measurements are performed at the output. However, even if the technique promises to achieve high precision, it depends on the decomposition of the signal based on the specific temporal structure of the incoming photon wavepacket, which increases the difficulty in the experimental implementation [10], and the presence of mode

crosstalk affects the sensitivity [11–15]. In the search of a new method which could enable the estimation problem in exam without the drawbacks of the current ones, we delve into the field of two-photon quantum interference, which has been a fruitful ground for many noteworthy results in quantum sensing [16–20]. In particular, in the celebrated Hong-Ou-Mandel quantum interference effect when two identical photons are sent to the two faces of a balanced beam splitter they will always bunch together at the same output port [16, 17]. Instead, when the two photons are not identical, there is a non-zero probability that a coincidence event could happen. Unfortunately, an estimation scheme solely based on this principle would require an overlap in time between the wavepackets of the two interfering photons, otherwise it would be insensitive to the parameter to estimate [21, 22]. However, new techniques based on multiphoton interference with inner variable boson sampling, which have first revealed an advantage in quantum computational complexity [23–26], have shown that it is possible to surpass these inconveniences, while at the same time reaching a precision equal to the quantum Cramér-Rao bound in the estimation of photonic parameters, such as time delays, polarisations, and displacements [21, 22, 27–30]. However, the exploration of novel two-photon interference techniques enabling the resolution in time of two incoherent signals beyond the Rayleigh limit in the time domain is yet largely terra incognita.

In this letter, we propose a new scheme for the estimation of the delay of two incoherent signals emitted by two weak thermal sources based on the quantum interference between a reference photon and one probe photon coming from either of the two weak sources, which overcomes the drawbacks of the aforementioned methods. We first demonstrate the unique quantum beat phenomena associated with the interference at a

* vincenzo.tamma@port.ac.uk

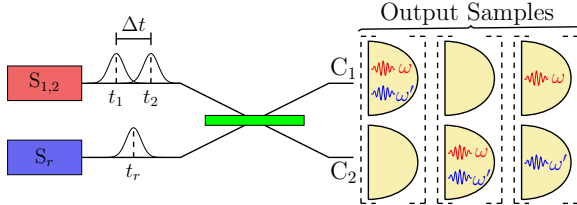


Figure 1. Two-photon interferometer. Two incoherent photons are emitted with a time delay Δt in the same line of sight, one of them interferes on a balanced beam splitter with a photon produced by a reference source. The possible outputs depend on the frequency of the detected photons and if they bunch together or hit different cameras. This scheme allows to retrieve the value of the time delay Δt with quantum-enhanced sensitivity and a relatively low number of measurements.

balanced beam splitter between the reference single photon and the probe photon in an incoherent superposition in the source emission times when they are collected by two cameras resolving their frequencies. We then exploit such interesting quantum phenomena to achieve quantum sensitivity in the measurement of the unknown time delay. Our method does not require the mode decomposition of the wavepackets of the incoming photons and it works independently of their shape. Furthermore, we demonstrate that for indistinguishable photons at the detectors our scheme achieves constant precision at half of the quantum limit in the estimation of the time delay independently of the value of the delay. The feasibility of our technique makes it an ideal candidate in many applications such as remote clock synchronization [31, 32], astronomical observations [33], spontaneous emission time measurements [8], condensed matter physics [34], or observation of incoherent scattering between photons in biological samples [35]. It can also be applied in those scenarios where an incoherent superposition in time of the signals arises from the interaction of a coherent laser pulse with two displaced objects in presence of turbulence between the two objects or in the case in which their distance is higher than the coherence length of the two wavepackets. As an example, a new method has been proposed for the radar ranging problem [36–38], which works by sending a signal to the two objects of interest and measuring the returning photons, relying on their coherence. However, in this case the associated quantum Fisher information vanishes quadratically when $\Delta t \rightarrow 0$, before even allowing perfect experimental conditions. Instead, by employing our technique an incoherent scattering with the two objects would be advantageous instead of being a limitation, and constant Fisher information, beyond the classical limit, could be reached even in the case of small delays and independently of any turbulence which may contribute

to generate incoherence [39–41].

Quantum interference of a single photon associated with two weak incoherent delayed signals and a reference photon As shown in Fig. 1 two incoherent weak signals propagate along the same line of sight separated by a time delay Δt . The associated quantum state in the single-photon regime, can be described by the density operator:

$$\hat{\rho} = \frac{1}{2} (|\psi_1\rangle\langle\psi_1| + |\psi_2\rangle\langle\psi_2|), \quad (1)$$

$$|\psi_i\rangle = \int_{\mathbb{R}} d\omega \xi_i(\omega) \hat{a}_1^\dagger(\omega) |\text{vac}\rangle, \quad i = 1, 2$$

with $\xi_i(\omega) = \bar{\xi}(\omega) e^{-i\omega t_i}$, $i = 1, 2$ the frequency probability amplitude of the photons, t_i the central time at which the i th photon hits the beam splitter, with the time delay $\Delta t = t_2 - t_1$ and the average time $t_s = (t_1 + t_2)/2$, while $\hat{a}_1^\dagger(\omega)$ is the bosonic creation operator associated with a photon with frequency ω . We notice that $|\psi_1\rangle$ and $|\psi_2\rangle$ are not orthogonal.

The probe photon emitted by the two incoherent sources impinges on one of the two faces of a balanced beam splitter, while a reference photon is injected at the other input of the beam splitter at central time t_r with state

$$|\psi_0\rangle = \int_{\mathbb{R}} d\omega \xi_0(\omega) \hat{d}_0^\dagger(\omega) |\text{vac}\rangle, \quad (2)$$

where $\hat{d}_0^\dagger(\omega)$ is the bosonic creation operator associated with a reference photon at the frequency ω , and $\xi_0 = \bar{\xi} e^{-i\omega t_r}$. The bosonic operators satisfy the commutation relations $[\hat{a}_S(\omega), \hat{d}_{S'}^\dagger(\omega')] = \sqrt{\nu} \delta_{S,S'} \delta(\omega - \omega')$, with $S, S' = 0, 1$, which means that we can rewrite $\hat{d}_S(\omega) = \sqrt{\nu} \hat{a}_S(\omega) + \sqrt{1-\nu} \hat{b}_S(\omega)$ with \hat{a} and \hat{b} orthogonal modes. Here, $0 \leq \nu \leq 1$ represents the degree of indistinguishability between photons in all physical degrees of freedom except for their arrival times, where $\nu = 1$ corresponds to complete indistinguishability. In all instances, the probability amplitudes in the frequency domain are such that $|\xi_0| = |\xi_1| = |\xi_2| = \bar{\xi}$.

After the interaction at the beam splitter, the detection is performed using two single-photon cameras positioned at the two output ports, allowing us to detect the frequencies ω, ω' of the two photons. A single measurement result, $(\Delta\omega, X)$, is defined by the difference in the frequency, $\Delta\omega = \omega - \omega'$, of the two photons and whether both photons impinge on the same camera ($X = B$, bunching event) or on different cameras ($X = A$, anti-bunching event).

In Appendix A we derive the probability

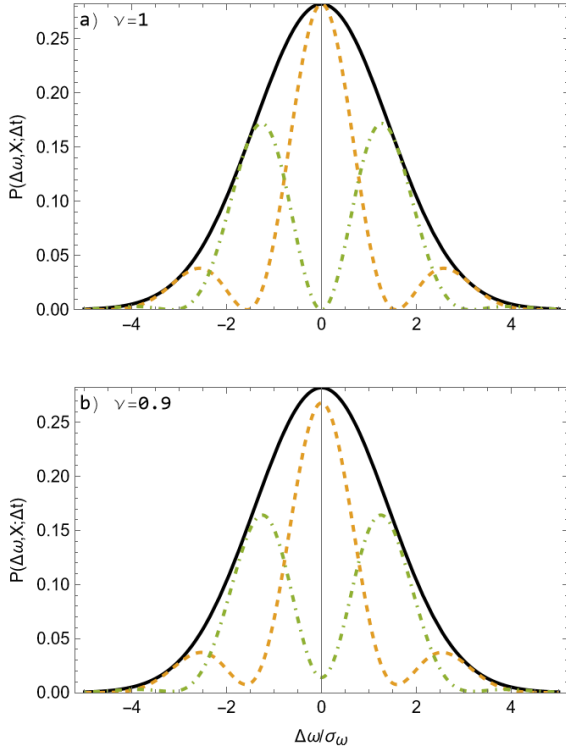


Figure 2. Quantum beat interference in the two-photon interferometer in Fig.1. Plots of the probability distribution $P(\Delta\omega, X; \Delta t)$ at the interferometer output given by the function in Eq. (4) of the frequency difference $\Delta\omega$, in units of the frequency bandwidth σ_ω , for a fixed time delay $\Delta t = 4/\sigma_\omega = 8\sigma_t$. Plot a) corresponds to indistinguishable photons, $\nu = 1$, and plot b) corresponds to partially distinguishable photons, $\nu = 0.9$. The coincidence probability ($X = A$) in the dashed-dotted green line, and the bunching probability ($X = B$) in the dashed orange line. The probability clearly manifests quantum beats with a periodicity inversely proportional to Δt .

$$P_\nu(\Delta\omega, X; \Delta t, t_r - t_s) = \frac{1}{2} \eta C(\Delta\omega) \times \left\{ 1 + \alpha(X) \nu \cos \left[\Delta\omega \frac{\Delta t}{2} \right] \cos [\Delta\omega(t_r - t_s)] \right\}, \quad (3)$$

where $\alpha(B) = 1$, $\alpha(A) = -1$, and $\eta < 1$ is a factor that accounts for detector losses, and $C(\Delta\omega)$ is an envelope function which shape is given by the frequency distribution, e.g., $C(\Delta\omega) = \exp(-\Delta\omega^2/4\sigma_\omega^2)/\sqrt{4\pi\sigma_\omega^2}$ in the case of a Gaussian frequency distribution $\xi(\omega)$ with variance $\sigma_\omega^2 = 1/4\sigma_t^2$, with σ_t^2 the variance of the corresponding photon temporal wavepacket. This probability describes the observation of a photon pair in the sampling outcome $(\Delta\omega, X)$ and depends on the time delay $\Delta t = t_1 - t_2$ and the time centroid $t_s = (t_1 + t_2)/2$ associated with the two incoherent signals. Importantly, this result indicates that two-photon interference beats

can be observed as a function of the frequency difference $\Delta\omega$.

If the two incoherent pulses do not experience any time delay, i.e. they are emitted at the same time, $\Delta t = 0$, the two-photon interference beatings in the probability in Eq. (3) are function of $\Delta\omega$ with a periodicity inversely proportional to the difference $(t_r - t_s)$ between the central time of emission t_r of the reference photon wave packet and the time centroid t_s of the probe signals. Here we will consider the case of signals emitted at different times, $\Delta t \neq 0$, and a reference photon with central arrival time at the beam splitter input given by the centroid time of the probe photon, which can be estimated through time resolved direct detection [10], so that $t_r = t_s$. In this regime, the quantum beats in the probability

$$P_\nu(\Delta\omega, X; \Delta t) = \frac{1}{2} \eta C(\Delta\omega) \times \left\{ 1 + \alpha(X) \nu \cos \left[\Delta\omega \frac{\Delta t}{2} \right] \right\}, \quad (4)$$

obtained from Eq. (3) under the condition $t_r = t_s$, exhibit a periodicity inversely proportional to the time delay Δt , as can be seen in Fig. 2. We aim to exploit this quantum feature of the scheme to estimate the time delay between the incoherent signals. Furthermore, since our measurement is carried out by resolving in the frequency, i.e. the conjugate variable of time, it is only necessary for the cameras to be able to resolve oscillations with a period $\propto 1/\Delta t$, bypassing the requirement of high precision in time, which is necessary in time-resolved direct detection methods.

Quantum estimation technique for indistinguishable photons We will now show that we can develop an efficient quantum metrological technique, harnessing two-photon quantum beats in the frequency domain, to estimate the time delay Δt , through sampling from the probability distribution given in Eq. (4). The estimation of Δt is done by recording the sampling outcomes $\{\Delta\omega, X\} = (\Delta\omega_i, X_i)$, with $i = 1, \dots, N$, obtained from N two-photon interference measurements, using the interferometer illustrated in Fig. 1, and using the gathered data to evaluate the maximum-likelihood estimator $\widehat{\Delta t}$. Remarkably, we now show that with our technique it is possible to accurately estimate the time delay, Δt , between the two photons even when it approaches zero. To this end, we evaluate the Cramér-Rao bound [6]

$$\text{Var}[\widehat{\Delta t}] \geq \frac{1}{N F_\nu(\Delta t)}, \quad (5)$$

which establishes the fundamental lower bound on the variance $\text{Var}[\widehat{\Delta t}]$ achievable using our metrological technique in a maximum likelihood estimation, with N representing the number of detected photon pairs, while $F_\nu(\Delta t)$ is the Fisher information corresponding to the frequency-resolved measurement scheme.

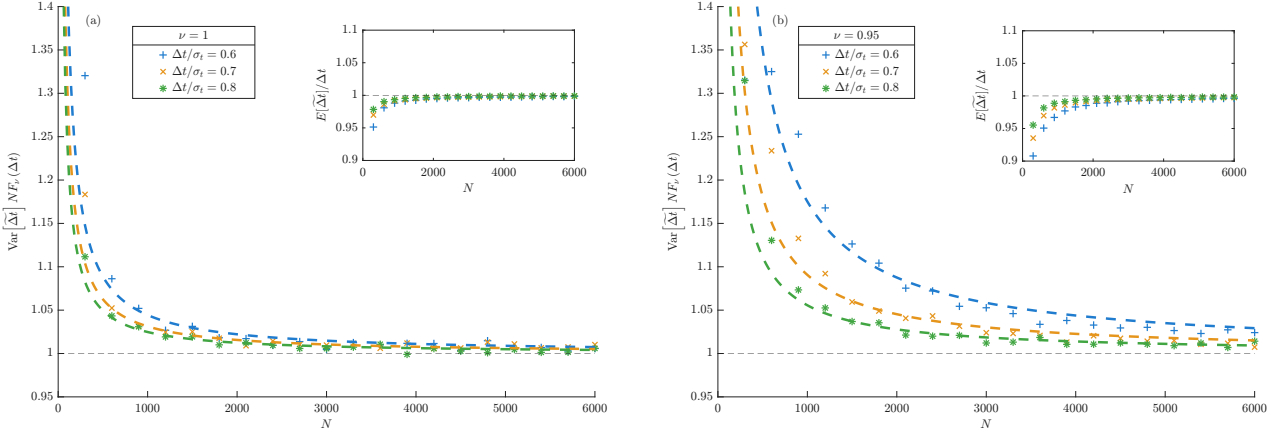


Figure 3. Numerical simulations for Gaussian wavepackets of the rate of convergence of the variance of the maximum likelihood estimator $\tilde{\Delta}t$ normalized to the Cramér-Rao bound in Eq. (5), for different numbers N of collected samples and for $\Delta t/\sigma_t = 0.6, 0.7, 0.8$, in the case of (a) indistinguishable photons, $\nu = 1$ (Fisher information $F_{\nu=1}$ in Eq. (6)), and (b) partially distinguishable photons, $\nu = 0.95$ (Fisher information in Eq. (8)). We show that the data can be fitted with the curve $1 + a/N$, where a/N is a correction term of order $1/N$ of the variance of the estimator normalized to the Cramér-Rao bound in Eq. (5) for $N \gg 1$. Thus showing that our scheme approaches the Cramér-Rao bound already for $N \simeq 5000$. In the insets, we also plot the estimated expectation value of the maximum-likelihood estimator normalized by its real value, showing that the estimation is unbiased already again for $N \simeq 5000$.

If we were to use time-resolved direct measurements for the estimation of Δt the Fisher information would vanish quadratically for $\Delta t \rightarrow 0$ even in ideal conditions such as unlimited time resolution, making it impossible to accurately estimate the parameter. Contrarily we now demonstrate that the Fisher Information for our technique is constant for every value of Δt , even when it approaches zero. In Appendix B we evaluate the Fisher information found in Eq. (5) for the probability distribution in Eq. (4), in the case of perfectly indistinguishable photons $\nu = 1$, obtaining

$$F_{\nu=1}(\Delta t) = \eta \frac{\sigma_{\omega}^2}{2} = \eta \frac{1}{8\sigma_t^2}, \quad (6)$$

which is directly proportional to the variance σ_{ω}^2 of the frequency distribution and inversely proportional to the variance σ_t^2 of the temporal wavepacket. Consequently, narrower temporal distributions lead to a higher achievable precision in the estimation of the time delay. Notably, the independence of $F(\Delta t)$ from Δt indicates that the estimation precision attainable with our two-photon interference scheme remains constant for all parameter values, irrespective of the photonic wavepacket structure. Furthermore, the Fisher Information differs from the quantum limit

$$Q(\Delta t) = \sigma_{\omega}^2 = \frac{1}{4\sigma_t^2} \quad (7)$$

only by the constant factor $\frac{1}{2}\eta$ [7]. To illustrate the significance of this result, consider a biphoton rate of

1 MHz with lossless detectors ($\eta = 1$). If photons with a temporal width $\sigma_t \sim 60$ fs are employed, which is achievable with current technology [42, 43], a timing precision of the order of attoseconds could be reached in only 4 h of measurement, and for a $\sigma_t \simeq 10$ fs, it would only take about 8 min to reach the same precision, making our method not only highly precise, but also remarkably fast. Furthermore our sampling scheme relies on a simple state-of-the-art optical apparatus and is independent of the specific shape of the wavepacket. It is therefore more experimentally feasible than other recent imaging techniques relying on demultiplexing, i.e. the decomposition of the incoming optical field into a basis of orthogonal modes dependent on the structure of the input wavepacket through the use of a specific waveguide, also wavepacket dependent, which by consequence renders the measurements affected by mode cross-talking [11, 12, 14, 15]. Furthermore, for photons with highly overlapping wavepackets, $\sigma_{\omega}\Delta t \ll 1$, we demonstrate in Appendix D that the same Fisher information given in Eq. (6) can be also attained relying solely on the sampling outcomes ($X = A, B$) on two simple bucket detectors. We estimate the parameter Δt by using standard maximum likelihood estimation. In particular, in Fig. 3 (a) are depicted the numerical simulations of the variance, $\text{var}(\tilde{\Delta}t)$, of the maximum likelihood estimator for a Gaussian wavepacket normalized by the Cramér-Rao bound in Eq. (5), and the expected value of the estimator, $E[\tilde{\Delta}t]$, normalized to the real value of the parameter Δt . The inset confirms the unbiased character of the

estimator, while the main graph displays a fit of the numerical data to the function $1 + a/N$, where a/N is the correction term of order $1/N$ of the variance normalized to the Cramér-Rao bound, as shown in the Appendix E. The parameters reported in Table I reveal that higher-order terms in $1/N$ are negligible. For $\nu = 1$ our method approaches the Cramér-Rao bound in Eq. (5), apart from a correction term a/N of order $\simeq 1\%$, already with $N \simeq 5000$ detected photon pairs as evident in Fig.3 (a).

$\nu = 1$			
$\Delta t/\sigma_t$	SSE	R^2	$a (a_{min}, a_{max})$
0.6	6.2531e-04	0.9150	44.34 (39.52, 49.15)
0.7	1.9697e-04	0.9178	31.26 (28.56, 33.96)
0.8	1.7529e-04	0.9216	24.79 (22.24, 27.34)
$\nu = 0.95$			
$\Delta t/\sigma_t$	SSE	R^2	$a (a_{min}, a_{max})$
0.6	0.0015	0.9429	175.2 (162.3, 188.1)
0.7	6.5066e-04	0.9161	90.64 (82.28, 99.01)
0.8	2.2080e-04	0.9070	55.6 (50.73, 60.47)

Table I. In this table we show the goodness of the fits plotted in Fig. 3, for indistinguishable photons ($\nu = 1$) and for partially distinguishable photons ($\nu = 0.95$). In the first column, we insert the values of the parameter to estimate in units of σ_t . For each of these values, we associate the summed square of residuals (SSE), the R-square (R^2), and the coefficient a , evaluated with 95% confidence (a_{min}, a_{max}).

Quantum estimation technique for partially distinguishable photons In experimental implementations, photons impinging on the detectors may exhibit partial distinguishability apart from the overlap in their temporal wavepacket, $\nu < 1$. Nonetheless, we can prove that the quantum advantage offered by our technique over time-resolved direct detection still remains. We consider for simplicity the case of Gaussian wavepackets with unitary σ_t .

In Appendix B we demonstrate that the Fisher information for our method, for $\nu < 1$, can be expressed as

$$F_\nu(\Delta t) = \frac{1}{4} \eta \int d\Delta\omega C(\Delta\omega) (\Delta\omega)^2 \times \frac{\nu^2 \sin^2 [\Delta\omega \Delta t / 2]}{1 - \nu^2 \cos^2 [\Delta\omega \Delta t / 2]}, \quad (8)$$

which, in the regime of large delays $\Delta t \gg \sigma_t$, approaches the constant value

$$F_\nu(\Delta t \gg \sigma_t) = \left(1 - \sqrt{1 - \nu^2}\right) F_{\nu=1}, \quad (9)$$

with $F_{\nu=1}$ in Eq. (6) as shown in Appendix C. Remarkably, this shows that the achievable precision in this regime is again constant and independent of the estimated parameter Δt , and increases for narrower temporal distributions. To prove the advantage of our method in Fig. 4 we compare the Fisher information in Eq.(8) with a realistic time-resolved direct-detection scenario in which the temporal resolution T is finite. We examine two different cases associated with temporal resolutions $T = 5\sigma_t$ and $T = 10\sigma_t$, which, although only assuming high resolution detectors with $T \approx 10^1\text{--}10^2$ ps [44, 45], can be relevant for example for photon scattering in biological tissue, where the detected field temporal width is in the picoseconds range and for thermal black-body radiation, whose coherence time is typically tens to hundreds of femtoseconds [46, 47]. As shown in Fig. 4, in both cases the Fisher information obtained from direct detection is lower than that achieved by our method, and already for $T = 10\sigma_t$ the classical approach becomes effectively unusable for any value of Δt given the vanishing Fisher information. Again, we show in Fig. 3 (b) that the estimator is unbiased and the convergence of the variance of the estimator to the Cramér-Rao bound apart from a correction term of the order $1/N$.

Conclusions The interferometric scheme we introduced in this work has the peculiar trait of manifesting the two-photon quantum beat interference phenomenon, which emerges from the frequency-resolved measurements of a single reference photon interfering with another photon from two incoherent weak signals. Moreover, we showed that this purely quantum feature is the basis upon which we can build a method to achieve for indistinguishable photons constant precision in the estimation of the time delay between the two incoherent signals, including the small delay regime in which classical time-resolved direct detection methods fail. Remarkably, this is possible by performing simple frequency-resolved sampling measurements from the output probability distribution of the photons. We also highlight that the achieved precision differs from the quantum limit only by a constant factor even when imperfect detectors are employed, and we can saturate the CRB already with a relatively low number of measurements. The advantage of the proposed scheme lies in its remarkable simplicity, which makes it possible to obtain constant precision without the complexities of the decomposition in orthogonal modes and the associated cross-talk drawbacks, maintaining the same efficiency independently of the value of the delay to estimate and of the photonic temporal wavepacket structure. Furthermore, we also showed that even for partially distinguishable pho-

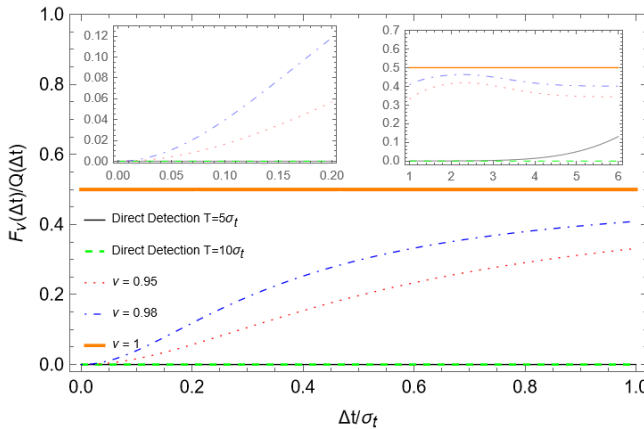


Figure 4. Plots of the Fisher information $F_\nu(\Delta t)$ in Eq. (8), for $\eta = 1$, and Fisher information for time-resolved direct detection as a function of the time delay $\Delta t/\sigma_t$, normalized by the Quantum Fisher information in Eq. (7), considering as an example a Gaussian temporal wavepacket with unitary σ_t . Direct detection in solid black line and dashed green line for a direct detection with resolution $T = 5\sigma_t$ and $T = 10\sigma_t$ respectively, F_ν in Eq. 8 in dotted red, $\nu = 0.95$, dot-dashed blue, $\nu = 0.98$, and thick solid orange, $\nu = 1$. In the left inset we show the same curves (constant function $F_{\nu=1}/Q = 1/2$ omitted here) for small delays, $0 < \Delta t/\sigma_t < 0.2$, while in the right inset we show them for large delays, $1 < \Delta t/\sigma_t < 6$, highlighting the clear advantage of our method in both regimes. In the right inset, it is also possible to observe the curves for $\nu \neq 1$ approaching the constant Fisher information value given in Eq. (9).

tons our technique can outperform classical detection, including the small delay regime. For its experimental feasibility this technique lends itself to important applications in astronomy, remote clock synchronization and radar ranging.

ACKNOWLEDGMENTS

We thank Paolo Facchi and Luca Maggio for the helpful discussions. This project was partially supported by the Air Force Office of Scientific Research under award number FA8655-23-1- 7046.

[1] Wolfgang Drexler and James G Fujimoto, *Optical coherence tomography: technology and applications* (Springer Science & Business Media, 2008).

[2] Miles Hansard, Seungkyu Lee, Ouk Choi, and Radu Patrice Horaud, *Time-of-flight cameras: principles, methods and applications* (Springer Science & Business Media, 2012).

[3] Peter W. Graham, Jason M. Hogan, Mark A. Kasevich, and Surjeet Rajendran, “New method for gravitational wave detection with atomic sensors,” *Phys. Rev. Lett.* **110**, 171102 (2013).

[4] D.J. Bradley, B. Liddy, and W.E. Sleat, “Direct linear measurement of ultrashort light pulses with a picosecond streak camera,” *Optics Communications* **2**, 391–395 (1971).

[5] Max Born, Emil Wolf, A. B. Bhatia, P. C. Clemmow, D. Gabor, A. R. Stokes, A. M. Taylor, P. A. Wayman, and W. L. Wilcock, *Principles of Optics: Electromagnetic Theory of Propagation, Interference and Diffraction of Light*, 7th ed. (Cambridge University Press, 1999).

[6] Harald Cramér, *Mathematical methods of statistics*, Vol. 9 (Princeton university press, 1999).

[7] Vahid Ansari, Benjamin Brecht, Jano Gil-Lopez, John M. Donohue, Jaroslav Řeháček, Zdeněk Hradil, Luis L. Sánchez-Soto, and Christine Silberhorn, “Achieving the ultimate quantum timing resolution,” *PRX Quantum* **2**, 010301 (2021).

[8] Cheyenne S. Mitchell and Mikael P. Backlund, “Quantum limits to resolution and discrimination of spontaneous emission lifetimes,” *Phys. Rev. A* **105**, 062603 (2022).

[9] Syamsundar De, Jano Gil-Lopez, Benjamin Brecht, Christine Silberhorn, Luis L. Sánchez-Soto, Zdeněk Hradil, and Jaroslav Řeháček, “Effects of coherence on temporal resolution,” *Phys. Rev. Res.* **3**, 033082 (2021).

[10] Ronakraj Ketan Gosalia and Robert Malaney, “Quantum-enhanced clock synchronization using prior statistical information,” *Quantum Science and Technology* (2025).

[11] Mankei Tsang, Ranjith Nair, and Xiao-Ming Lu, “Quantum theory of superresolution for two incoherent optical point sources,” *Phys. Rev. X* **6**, 031033 (2016).

[12] Martin Paúr, Bohumil Stoklasa, Zdeněk Hradil, Luis L. Sánchez-Soto, and Jaroslav Rehacek, “Achieving the ultimate optical resolution,” *Optica* **3**, 1144–1147 (2016).

[13] Tomasz Linowski, Konrad Schlichtholz, Giacomo Sorelli, Manuel Gessner, Mattia Walschaers, Nicolas Treps, and Lukasz Rudnicki, “Application range of crosstalk-affected spatial demultiplexing for resolving

separations between unbalanced sources," *New Journal of Physics* **25**, 103050 (2023).

[14] Luigi Santamaria, Deborah Pallotti, Mario Siciliani de Cumis, Daniele Dequal, and Cosmo Lupo, "Spatial-mode demultiplexing for enhanced intensity and distance measurement," *Opt. Express* **31**, 33930–33944 (2023).

[15] Luigi Santamaria, Fabrizio Sgobba, and Cosmo Lupo, "Single-photon sub-rayleigh precision measurements of a pair of incoherent sources of unequal intensity," *Optica Quantum* **2**, 46–56 (2024).

[16] C. K. Hong, Z. Y. Ou, and L. Mandel, "Measurement of subpicosecond time intervals between two photons by interference," *Phys. Rev. Lett.* **59**, 2044–2046 (1987).

[17] Y. H. Shih and C. O. Alley, "New type of einstein-podolsky-rosen-bohm experiment using pairs of light quanta produced by optical parametric down conversion," *Phys. Rev. Lett.* **61**, 2921–2924 (1988).

[18] Ashley Lyons, George C. Knee, Eliot Bolduc, Thomas Roger, Jonathan Leach, Erik M. Gauger, and Daniele Faccio, "Attosecond-resolution hong-ou-mandel interferometry," *Science Advances* **4**, 5 (2018).

[19] Natapon Harnchaiwat, Feng Zhu, Niclas Westerberg, Erik Gauger, and Jonathan Leach, "Tracking the polarisation state of light via hong-ou-mandel interferometry," *Opt. Express* **28**, 2210–2220 (2020).

[20] Fabrizio Sgobba, Deborah Katia Pallotti, Arianna Elefante, Stefano Dello Russo, Daniele Dequal, Mario Siciliani de Cumis, and Luigi Santamaria Amato, "Optimal measurement of telecom wavelength single photon polarisation via hong-ou-mandel interferometry," *Photonics* **10** (2023), 10.3390/photonics10010072.

[21] Danilo Triggiani, Giorgos Psaroudis, and Vincenzo Tamma, "Ultimate quantum sensitivity in the estimation of the delay between two interfering photons through frequency-resolving sampling," *Phys. Rev. Appl.* **19**, 044068 (2023).

[22] Danilo Triggiani and Vincenzo Tamma, "Estimation with ultimate quantum precision of the transverse displacement between two photons via two-photon interference sampling measurements," *Phys. Rev. Lett.* **132**, 180802 (2024).

[23] Vincenzo Tamma and Simon Laibacher, "Multiboson correlation interferometry with arbitrary single-photon pure states," *Physical review letters* **114**, 243601 (2015).

[24] Xu-Jie Wang, Bo Jing, Peng-Fei Sun, Chao-Wei Yang, Yong Yu, Vincenzo Tamma, Xiao-Hui Bao, and Jian-Wei Pan, "Experimental time-resolved interference with multiple photons of different colors," *Physical review letters* **121**, 080501 (2018).

[25] Simon Laibacher and Vincenzo Tamma, "Symmetries and entanglement features of inner-mode-resolved correlations of interfering nonidentical photons," *Physical Review A* **98**, 053829 (2018).

[26] Vincenzo Tamma and Simon Laibacher, "Multiboson correlation interferometry with multimode thermal sources," *Physical Review A* **90**, 063836 (2014).

[27] L. Maggio, D. Triggiani, P. Facchi, and V. Tamma, "Multi-parameter estimation of the state of two interfering photonic qubits," (2024), arXiv:2405.12870 [quant-ph].

[28] Thomas Legero, Tatjana Wilk, Markus Hennrich, Gerhard Rempe, and Axel Kuhn, "Quantum beat of two single photons," *Physical review letters* **93**, 070503 (2004).

[29] Thomas Legero, Tatjana Wilk, Axel Kuhn, and Gerhard Rempe, "Time-resolved two-photon quantum interference," *Applied Physics B* **77**, 797–802 (2003).

[30] Salvatore Muratore, Danilo Triggiani, and Vincenzo Tamma, "Superresolution imaging of two incoherent sources via two-photon-interference sampling measurements of the transverse momenta," *Phys. Rev. Appl.* **23**, 054033 (2025).

[31] Fabrizio R Giorgetta, William C Swann, Laura C Sinclair, Esther Baumann, Ian Coddington, and Nathan R Newbury, "Optical two-way time and frequency transfer over free space," *Nature Photonics* **7**, 434–438 (2013).

[32] W. Gao, S.W. Kim, H. Bosse, H. Haitjema, Y.L. Chen, X.D. Lu, W. Knapp, A. Weckenmann, W.T. Estler, and H. Kunzmann, "Measurement technologies for precision positioning," *CIRP Annals* **64**, 773–796 (2015).

[33] P Krehlik, J Kolodziej, M Lipiński, J Nawrocki, P Nogaś, A Marecki, E Pazderski, P Ablewski, M Bober, R Ciuryło, *et al.*, "Fibre-optic delivery of time and frequency to vlbi station," *Astronomy & Astrophysics* **603**, A48 (2017).

[34] Ferenc Krausz and Misha Ivanov, "Attosecond physics," *Rev. Mod. Phys.* **81**, 163–234 (2009).

[35] Bingying Chen, Tonmoy Chakraborty, Stephan Daetwyler, James D Manton, Kevin Dean, and Reto Fiolk, "Extended depth of focus multiphoton microscopy via incoherent pulse splitting," *Biomedical Optics Express* **11**, 3830–3842 (2020).

[36] Andrew N. Jordan and John C. Howell, "Fundamental limits on subwavelength range resolution," *Phys. Rev. Appl.* **20**, 064046 (2023).

[37] Andrew N. Jordan, John C. Howell, Achim Kempf, Shunxing Zhang, and Derek White, "Optimal radar ranging pulse to resolve two reflectors," *Phys. Rev. Res.* **6**, 033341 (2024).

[38] John C. Howell, Andrew N. Jordan, Barbara Šoda, and Achim Kempf, "Super interferometric range resolution," *Phys. Rev. Lett.* **131**, 053803 (2023).

[39] Azezigul Abdulkirim, Yichong Ren, Zhiwei Tao, Shiwei Liu, Yanling Li, Hanling Deng, and Ruizhong Rao, "Effects of atmospheric coherent time on inverse synthetic aperture radar imaging through atmospheric turbulence," *Remote Sensing* **15**, 2883 (2023).

[40] Changqing Cao, Xiyuan Su, Yutao Liu, Xiaodong Zeng, Zhejun Feng, Jingshi Shen, Ting Wang, and Xu Yan, "Compensation for the decoherence effect in heterodyne detection of rough targets and a target vibration characteristic measurement system," *Scientific Reports* **10**, 6077 (2020).

[41] Jiyu Xue, Yunhua Cao, Zhensen Wu, Yanhui Li, Geng Zhang, Kai Yang, and Ruoting Gao, "Inverse synthetic aperture lidar imaging and compensation in slant atmospheric turbulence with phase gradient algorithm compensation," *Optics & Laser Technology* **154**, 108329 (2022).

[42] Peter J Mosley, Jeff S Lundeen, Brian J Smith, Piotr Wasylczyk, Alfred B U'Ren, \downarrow ? format? \downarrow Christine Silberhorn, and Ian A Walmsley, "Heralded generation of

ultrafast single photons in pure quantum states," Physical Review Letters **100**, 133601 (2008).

[43] Magued B Nasr, Silvia Carrasco, Bahaa EA Saleh, Alexander V Sergienko, Malvin C Teich, Juan P Torres, Lluis Torner, David S Hum, and Martin M Fejer, "Ultrabroadband biphotons generated via chirped quasi-phase-matched optical parametric down-conversion," Physical review letters **100**, 183601 (2008).

[44] Boris Korzh, Qing-Yuan Zhao, Jason P Allmaras, Simone Frasca, Travis M Autry, Eric A Bersin, Andrew D Beyer, Ryan M Briggs, Bruce Bumble, Marco Colangelo, *et al.*, "Demonstration of sub-3 ps temporal resolution with a superconducting nanowire single-photon detector," Nature Photonics **14**, 250–255 (2020).

[45] W Gao, Seung-Woo Kim, H Bosse, H Haitjema, YL Chen, XD Lu, W Knapp, A Weckenmann, WT Essler, and H Kunzmann, "Measurement technologies for precision positioning," CIRP annals **64**, 773–796 (2015).

[46] Oybek Kholiqov, Wenjun Zhou, Tingwei Zhang, VN Du Le, and Vivek J Srinivasan, "Time-of-flight resolved light field fluctuations reveal deep human tissue physiology," Nature communications **11**, 391 (2020).

[47] Berke Vow Ricketti, Erik M Gauger, and Alessandro Fedrizzi, "The coherence time of sunlight in the context of natural and artificial light-harvesting," Scientific Reports **12**, 5438 (2022).

Appendix A: Probability in Eq. (3)

Here we derive the expression for the probability $P_\nu(\Delta\omega, X; \Delta t, t_r - t_s)$ in Eq. 3 in the main text, of measuring the photons with frequencies ω, ω' , when they hit the same camera ($X = B$, bunching event) or different cameras ($X = A$, antibunching event).

We can describe the action of the beam splitter on the incoming photons via a 2×2 unitary matrix U_{BS}

$$U_{BS} = \frac{1}{\sqrt{2}} \begin{pmatrix} 1 & -1 \\ 1 & 1 \end{pmatrix}, \quad (\text{A1})$$

which transforms the creation operators through the map $\hat{U}_{BS}\hat{a}_i^\dagger\hat{U}_{BS}^\dagger = \sum_{j=0,1}(U_{BS})_{ij}\hat{a}_j^\dagger$, and analogously for \hat{b}_i^\dagger . So we can define the state at the output of the beam-splitter as

$$\begin{aligned} \hat{\rho}' &= \hat{U}_{BS}\hat{\rho}\hat{U}_{BS}^\dagger = \frac{1}{2} \left[\hat{U}_{BS} |\psi_0\rangle\langle\psi_0| \otimes |\psi_1\rangle\langle\psi_1| \hat{U}_{BS}^\dagger + \hat{U}_{BS} |\psi_0\rangle\langle\psi_0| \otimes |\psi_2\rangle\langle\psi_2| \hat{U}_{BS}^\dagger \right] \\ &= \sum_{i=1,2} \frac{1}{8} \int_{\mathbb{R}^2} d\omega_0 d\omega_i \xi_0(\omega_0) \xi_i(\omega_i) \left[\sqrt{\nu} \left(\hat{a}_{0,\omega_0}^\dagger - \hat{a}_{1,\omega_0}^\dagger \right) + \sqrt{1-\nu} \left(\hat{b}_{0,\omega_0}^\dagger - \hat{b}_{1,\omega_0}^\dagger \right) \right] \left(\hat{a}_{0,\omega_i}^\dagger + \hat{a}_{1,\omega_i}^\dagger \right) |\text{vac}\rangle\langle\text{vac}| \\ &\quad \times \int_{\mathbb{R}^2} d\omega'_0 d\omega'_i \xi_0^*(\omega'_0) \xi_i^*(\omega'_i) \left[\sqrt{\nu} \left(\hat{a}_{0,\omega_0} - \hat{a}_{1,\omega_0} \right) + \sqrt{1-\nu} \left(\hat{b}_{0,\omega_0} - \hat{b}_{1,\omega_0} \right) \right] \left(\hat{a}_{0,\omega_i} + \hat{a}_{1,\omega_i} \right) \end{aligned} \quad (\text{A2})$$

after the evolution through the beam splitter of the initial state expressed by the density operator $\hat{\rho} = \frac{1}{2} |\psi_0\rangle\langle\psi_0| \otimes (|\psi_1\rangle\langle\psi_1| + |\psi_2\rangle\langle\psi_2|)$, with $|\psi_1\rangle, |\psi_2\rangle$ given by Eq.(1) in the main text. To evaluate the probability of either a coincidence or a bunching event after the photons hit the beam splitter, we manipulate the integral to better analyse the contribution of the distinguishability between photons, so

$$\begin{aligned} \rho' &= \frac{1}{8} \sum_{i=1,2} \left\{ \sqrt{\nu} \int_{\omega_0 < \omega_i} d\omega_0 d\omega_i [\xi_0(\omega_0)\xi_i(\omega_i) + \xi_0(\omega_i)\xi_i(\omega_0)] [\hat{a}_{0,\omega_0}^\dagger \hat{a}_{0,\omega_i}^\dagger - \hat{a}_{1,\omega_0}^\dagger \hat{a}_{1,\omega_i}^\dagger] \right. \\ &\quad + \sqrt{\nu} \int_{\omega_0 < \omega_i} d\omega_0 d\omega_i [\xi_0(\omega_0)\xi_i(\omega_i) - \xi_0(\omega_i)\xi_i(\omega_0)] [\hat{a}_{0,\omega_0}^\dagger \hat{a}_{1,\omega_i}^\dagger - \hat{a}_{1,\omega_0}^\dagger \hat{a}_{0,\omega_i}^\dagger] \\ &\quad + \sqrt{1-\nu} \int_{\mathbb{R}^2} d\omega_0 d\omega_i \xi_0(\omega_0) \xi_i(\omega_i) [\hat{b}_{0,\omega_0}^\dagger \hat{a}_{0,\omega_i}^\dagger - \hat{b}_{1,\omega_0}^\dagger \hat{a}_{1,\omega_i}^\dagger + \hat{b}_{0,\omega_0}^\dagger \hat{a}_{1,\omega_i}^\dagger - \hat{b}_{1,\omega_0}^\dagger \hat{a}_{0,\omega_i}^\dagger] \Big\} |\text{vac}\rangle\langle\text{vac}| \\ &\quad \left\{ \sqrt{\nu} \int_{\omega_0 < \omega_i} d\omega_0 d\omega_i [\xi_0(\omega_0)\xi_i(\omega_i) + \xi_0(\omega_i)\xi_i(\omega_0)] [\hat{a}_{0,\omega_0} \hat{a}_{0,\omega_i} - \hat{a}_{1,\omega_0} \hat{a}_{1,\omega_i}] \right. \\ &\quad + \sqrt{\nu} \int_{\omega_0 < \omega_i} d\omega_0 d\omega_i [\xi_0(\omega_0)\xi_i(\omega_i) - \xi_0(\omega_i)\xi_i(\omega_0)] [\hat{a}_{0,\omega_0} \hat{a}_{1,\omega_i} - \hat{a}_{1,\omega_0} \hat{a}_{0,\omega_i}] \\ &\quad \left. + \sqrt{1-\nu} \int_{\mathbb{R}^2} d\omega_0 d\omega_i \xi_0(\omega_0) \xi_i(\omega_i) [\hat{b}_{0,\omega_0} \hat{a}_{0,\omega_i} - \hat{b}_{1,\omega_0} \hat{a}_{1,\omega_i} + \hat{b}_{0,\omega_0} \hat{a}_{1,\omega_i} - \hat{b}_{1,\omega_0} \hat{a}_{0,\omega_i}] \right\} \end{aligned} \quad (\text{A3})$$

in which we can interpret the first and second contributes as the outcomes in which the photons bunch together or end up in a different channel respectively, the third instead represents the case in which some distinguishability in

the inner properties of the two photons, aside from time and frequency, is observed at the detector. Now it is possible to easily evaluate the probabilities relative either to a bunching or an antibunching event. First we calculate the probability $p_B ([\omega - \delta\omega/2, \omega + \delta\omega/2], [\omega' - \delta\omega/2, \omega' + \delta\omega/2])$ to observe the two photons bunching together with frequencies ω, ω' within the resolution $\delta\omega$

$$\begin{aligned}
& p_B ([\omega - \delta\omega/2, \omega + \delta\omega/2], [\omega' - \delta\omega/2, \omega' + \delta\omega/2]) \\
&= \int_{\omega - \delta\omega/2}^{\omega + \delta\omega/2} \int_{\omega' - \delta\omega/2}^{\omega' + \delta\omega/2} dw_1 dw_2 \sum_{j=0,1} \left[\langle \text{vac} | \hat{a}_{j,w_1} \hat{a}_{j,w_2} \hat{\rho}' \hat{a}_{j,w_1}^\dagger \hat{a}_{j,w_2}^\dagger | \text{vac} \rangle + \langle \text{vac} | \hat{a}_{j,w_1} \hat{b}_{j,w_2} \hat{\rho}' \hat{a}_{j,w_1}^\dagger \hat{b}_{j,w_2}^\dagger | \text{vac} \rangle \right. \\
&\quad \left. + \langle \text{vac} | \hat{b}_{j,w_1} \hat{a}_{j,w_2} \hat{\rho}' \hat{b}_{j,w_1}^\dagger \hat{a}_{j,w_2}^\dagger | \text{vac} \rangle \right] \\
&= \frac{1}{2} \sum_{i=1,2} \int_{\omega - \delta\omega/2}^{\omega + \delta\omega/2} \int_{\omega' - \delta\omega/2}^{\omega' + \delta\omega/2} dw_1 dw_2 \left\{ \frac{\nu}{2} |\xi_0(w_1)\xi_i(w_2) + \xi_0(w_2)\xi_i(w_1)|^2 + \frac{1-\nu}{2} [|\xi_0(w_1)\xi_i(w_2)|^2 + |\xi_0(w_2)\xi_i(w_1)|^2] \right\} \\
&= \frac{1}{2} \sum_{i=1,2} \frac{1}{2} \left\{ |\xi_0(\omega)\xi_i(\omega')|^2 + |\xi_0(\omega')\xi_i(\omega)|^2 + 2\nu \text{Re} [\xi_0(\omega)\xi_i(\omega')\xi_0^*(\omega')\xi_i^*(\omega)] \right\} \delta\omega \delta\omega' \equiv p_B(\omega, \omega') \delta\omega^2,
\end{aligned} \tag{A4}$$

we assumed in the last step that $\delta\omega$ is small enough that we can neglect the variations of the integrand in the interval. The same can be done to evaluate the probability of a coincidence event

$$\begin{aligned}
& p_A ([\omega - \delta\omega/2, \omega + \delta\omega/2], [\omega' - \delta\omega/2, \omega' + \delta\omega/2]) \\
&= \int_{\omega - \delta\omega/2}^{\omega + \delta\omega/2} \int_{\omega' - \delta\omega/2}^{\omega' + \delta\omega/2} dw_1 dw_2 \left[\langle \text{vac} | \hat{a}_{0,w_1} \hat{a}_{1,w_2} \hat{\rho}' \hat{a}_{0,w_1}^\dagger \hat{a}_{1,w_2}^\dagger | \text{vac} \rangle + \langle \text{vac} | \hat{a}_{0,w_2} \hat{a}_{1,w_1} \hat{\rho}' \hat{a}_{0,w_2}^\dagger \hat{a}_{1,w_1}^\dagger | \text{vac} \rangle + \right. \\
&\quad \left. \langle \text{vac} | \hat{a}_{0,w_1} \hat{b}_{1,w_2} \hat{\rho}' \hat{a}_{0,w_1}^\dagger \hat{b}_{1,w_2}^\dagger | \text{vac} \rangle + \langle \text{vac} | \hat{a}_{0,w_2} \hat{b}_{1,w_1} \hat{\rho}' \hat{a}_{0,w_2}^\dagger \hat{b}_{1,w_1}^\dagger | \text{vac} \rangle + \langle \text{vac} | \hat{b}_{0,w_1} \hat{a}_{1,w_2} \hat{\rho}' \hat{b}_{0,w_1}^\dagger \hat{a}_{1,w_2}^\dagger | \text{vac} \rangle + \right. \\
&\quad \left. \langle \text{vac} | \hat{b}_{0,w_2} \hat{a}_{1,w_1} \hat{\rho}' \hat{b}_{0,w_2}^\dagger \hat{a}_{1,w_1}^\dagger | \text{vac} \rangle \right] \\
&= \frac{1}{2} \sum_{i=1,2} \int_{\omega - \delta\omega/2}^{\omega + \delta\omega/2} \int_{\omega' - \delta\omega/2}^{\omega' + \delta\omega/2} dw_1 dw_2 \left\{ \frac{\nu}{2} |\xi_0(w_1)\xi_i(w_2) - \xi_0(w_2)\xi_i(w_1)|^2 + \frac{1-\nu}{2} [|\xi_0(w_1)\xi_i(w_2)|^2 + |\xi_0(w_2)\xi_i(w_1)|^2] \right\} \\
&= \frac{1}{2} \sum_{i=1,2} \frac{1}{2} \left\{ |\xi_0(\omega)\xi_i(\omega')|^2 + |\xi_0(\omega')\xi_i(\omega)|^2 - 2\nu \text{Re} [\xi_0(\omega)\xi_i(\omega')\xi_0^*(\omega')\xi_i^*(\omega)] \right\} \delta\omega \delta\omega' \equiv p_A(\omega, \omega') \delta\omega^2.
\end{aligned} \tag{A5}$$

We suppose now that the frequency distributions are of the form $\xi_i(\omega) = \bar{\xi}(\omega)e^{-i\omega t_i}$, with $\bar{\xi}(\omega)$ real and independent on t_i , introduce the variables $\Omega = (\omega + \omega')/2$ and $\Delta\omega = (\omega - \omega')$, and then perform the integration over Ω , so we can rewrite

$$P(\Delta\omega, X; t_r, t_1, t_2) = \frac{1}{2} C(\Delta\omega) \left\{ 1 + \frac{1}{2} \alpha(X) \nu [\cos [\Delta\omega (t_r - t_1)] + \cos [\Delta\omega (t_r - t_2)]] \right\} \tag{A6}$$

where $\alpha(X) = +1$ for a bunching event and $\alpha(X) = -1$ for an antibunching event, and we defined the envelope function $C(\Delta\omega) = \int_{\mathbb{R}} d\Omega \bar{\xi}^2(\Omega + \Delta\omega/2) \bar{\xi}^2(\Omega - \Delta\omega/2)$, extending the integration domains over whole plane and consequently multiplying by the factor $\frac{1}{2}$ to normalize the probability. After the change of parameters $\Delta t = t_1 - t_2$ and $t_s = (t_1 + t_2)/2$ and taking into account the losses with a factor $\eta < 1$, it is possible to write Eq. (A6) as shown in Eq. (3) in the main text, i.e.

$$P(\Delta\omega, X; \Delta t, t_r - t_s) = \frac{1}{2} \eta C(\Delta\omega) \{ 1 + \alpha(X) \nu \cos [\Delta\omega \Delta t/2] \cos [\Delta\omega (t_r - t_s)] \} \tag{A7}$$

Appendix B: Fisher Information in Eqs. (6) and (8)

In this appendix we will evaluate the Cramér-Rao bound shown in Eq. (5) with the Fisher information shown in Eq. (6) in the main text. To do so, we will initially assume that both the parameters Δt and t_s associated with the

two sources are unknown, and show that the estimation of Δt is statistically independent from the estimation of t_s for a setup with $t_r - t_s = 0$, for which we evaluate the Fisher information $F(\Delta t)$.

The elements of a generic Fisher information matrix F associated with the estimation of any number p of parameters φ from a probability distribution $P(\mathbf{x}; \varphi)$ can be calculated as [6]

$$F_{ij} = \int d\mathbf{x} \frac{1}{P(\mathbf{x}; \varphi)} \left(\frac{\partial}{\partial \varphi_i} P(\mathbf{x}; \varphi) \right) \left(\frac{\partial}{\partial \varphi_j} P(\mathbf{x}; \varphi) \right), \quad i, j \in \{1, \dots, p\}. \quad (\text{B1})$$

In our estimation problem there are two parameters, Δt and t_s , so the Fisher information matrix is a 2x2 matrix, of which we can derive the elements applying the expression of the probability in Eq. (3) to Eq. (B1). The diagonal term relative to the estimation of Δt reads

$$F_{11} = \sum_{X=A,B} \int d\Delta\omega P(\Delta\omega, X; \Delta t, t_r - t_s) \left\{ \frac{d}{d\Delta t} \log [P(\Delta\omega, X; \Delta t, t_r - t_s)] \right\}^2 = \int d\Delta\omega f_{11}(\Delta\omega; \Delta t, t_r - t_s). \quad (\text{B2})$$

As we evaluate the derivative to be

$$\frac{d}{d\Delta t} P(\Delta\omega, X; \Delta t, t_r - t_s) = \frac{1}{2} \eta C(\Delta\omega) \alpha(X) \nu \left(-\frac{\Delta\omega}{2} \right) \sin [\Delta\omega \Delta t / 2] \cos [\Delta\omega (t_r - t_s)], \quad (\text{B3})$$

we can ultimately write the integrand $f_{11}(\Delta\omega; \Delta t, t_s)$ as

$$f_{11}(\Delta\omega; \Delta t, t_r - t_s) = \eta C(\Delta\omega) \frac{\Delta\omega^2}{4} \frac{\nu^2 \sin^2 [\Delta\omega \Delta t / 2] \cos^2 [\Delta\omega (t_r - t_s)]}{1 - \nu^2 \cos^2 [\Delta\omega \Delta t / 2] \cos^2 [\Delta\omega (t_r - t_s)]}. \quad (\text{B4})$$

Similarly, for the off-diagonal terms we obtain

$$F_{12} = F_{21} = \int d\Delta\omega f_{12}(\Delta\omega; \Delta t, t_r - t_s), \quad (\text{B5})$$

evaluating the derivative with respect to the centroid

$$\frac{d}{dt_s} P(\Delta\omega, X; \Delta t, t_r - t_s) = \frac{1}{2} \eta C(\Delta\omega) \alpha(X) \nu(\Delta\omega) \cos [\Delta\omega \Delta t / 2] \sin [\Delta\omega (t_r - t_s)] \quad (\text{B6})$$

the integrand is:

$$f_{12}(\Delta\omega; \Delta t, t_r - t_s) = -\eta C(\Delta\omega) \frac{(\Delta\omega)^2}{8} \frac{\nu^2 \sin [\Delta\omega \Delta t] \sin [2\Delta\omega (t_r - t_s)]}{1 - \nu^2 \cos^2 [\Delta\omega \Delta t / 2] \cos^2 [\Delta\omega (t_r - t_s)]} \quad (\text{B7})$$

And last the element relative to the centroid t_s is given by

$$F_{22} = \int d\Delta\omega f_{22}(\Delta\omega; \Delta t, t_r - t_s) \quad (\text{B8})$$

with:

$$f_{22}(\Delta\omega; \Delta t, t_r - t_s) = \eta C(\Delta\omega) (\Delta\omega)^2 \frac{\nu^2 \cos^2 [\Delta\omega \Delta t / 2] \sin^2 [\Delta\omega (t_r - t_s)]}{1 - \nu^2 \cos^2 [\Delta\omega \Delta t / 2] \cos^2 [\Delta\omega (t_r - t_s)]}. \quad (\text{B9})$$

If we now assume that the time t_r for the reference photon coincide with the time centroid, i.e. for $t_r = t_s$, the only non-vanishing integrand is $f_{11}(\Delta\omega; \Delta t, t_s)$, so that the Fisher information matrix reduces to a diagonal matrix

$$F = \begin{pmatrix} \frac{1}{4} \eta \int d\Delta\omega C(\Delta\omega) (\Delta\omega)^2 \frac{\nu^2 \sin^2 [\Delta\omega \Delta t / 2]}{1 - \nu^2 \cos^2 [\Delta\omega \Delta t / 2]} & 0 \\ 0 & 0 \end{pmatrix}, \quad (\text{B10})$$

which corresponds to the Fisher information in Eq.(8) in the main text for the estimation of Δt . In the case of completely indistinguishable photons, $\nu = 1$

$$F = \begin{pmatrix} \frac{1}{4} \eta \int d\Delta\omega C(\Delta\omega) (\Delta\omega)^2 & 0 \\ 0 & 0 \end{pmatrix} = \begin{pmatrix} \frac{\eta \sigma_\omega^2}{2} & 0 \\ 0 & 0 \end{pmatrix} = \begin{pmatrix} \frac{\eta}{8\sigma_t^2} & 0 \\ 0 & 0 \end{pmatrix}, \quad (\text{B11})$$

where σ_ω^2 and σ_t^2 are the variance of the frequency distribution of the photons and the variance of the temporal distribution of the photons respectively. This means that the estimation of Δt is statistically independent of t_s , and the Cramér-Rao bound for the estimation of Δt coincides with the Fisher information in Eq. (6) in the main text.

Appendix C: Fisher information for $\Delta t \gg \sigma_t$

In this section we derive the Fisher information in Eq. (9) in the main text by studying the behaviour of $F_\nu(\Delta t)$ for large time delays $\Delta t \gg \sigma_t$. We consider the expression in Eq. (B10). The integrand can be written as the product of two distinct contributions, a term dependent on the envelope, $C(\Delta\omega)(\Delta\omega)^2$, and a periodic function of $\Delta\omega$ with period $2\pi/\Delta t$,

$$\kappa_\nu(\Delta\omega\Delta t) = \frac{\nu^2 \sin^2(\Delta\omega\Delta t/2)}{1 - \nu^2 \cos^2(\Delta\omega\Delta t/2)}. \quad (\text{C1})$$

When the envelope varies slowly over a period $2\pi/\Delta t$, the first contribution to the integrand can be treated as approximately constant within each period. This condition is satisfied in the regime $\Delta t \gg \sigma_t$, for which the period $2\pi/\Delta t$ is much smaller than the frequency bandwidth $\sigma_\omega = 1/2\sigma_t$. In this case, we can compute the average of $\kappa_\nu(\Delta\omega\Delta t)$ over one period,

$$\frac{\Delta t}{2\pi} \int_0^{2\pi/\Delta t} d\Delta\omega \kappa_\nu(\Delta\omega\Delta t) = 1 - \sqrt{1 - \nu^2}. \quad (\text{C2})$$

Substituting this result into Eq. (B10), we obtain

$$F_\nu(\Delta t \gg \sigma_t) = (1 - \sqrt{1 - \nu^2}) F_{\nu=1}, \quad (\text{C3})$$

which coincides with Eq. (9) in the main text.

Appendix D: Fisher information for measurements not resolving the frequency

The already discussed experimental set-up includes two resolving cameras at the outputs of the beam splitter, now we consider to replace them with two bucket detectors which cannot resolve the frequency of the photons ω, ω' . The only information we can get is whether the photons are detected by the same ($X = B$) or different ($X = A$) detectors, happening with probabilities:

$$P(X) = \int d\Delta\omega P(\Delta\omega, X; \Delta t) = \frac{1}{2}\eta \left\{ 1 + \alpha(X) \int d\Delta\omega C(\Delta\omega) \cos\left(\Delta\omega \frac{\Delta t}{2}\right) \right\}, \quad (\text{D1})$$

obtained by the probability in Eq. (3) imposing that $t_r = t_s$.

By summing over the two possible outcomes $X = A, B$ we obtain:

$$\begin{aligned} F^{(nr)}(\Delta t) &= \sum_{A,B} P(X) \left(\frac{d}{d\Delta t} \log P(X) \right)^2 = \sum_{A,B} \frac{1}{2}\eta \frac{\left(\int d\Delta\omega C(\Delta\omega) \frac{\Delta\omega}{2} \sin\left(\Delta\omega \frac{\Delta t}{2}\right) \right)^2}{\left\{ 1 + \alpha(X) \int d\Delta\omega C(\Delta\omega) \cos\left(\Delta\omega \frac{\Delta t}{2}\right) \right\}} \\ &= \times \frac{1}{4}\eta \frac{\left(\int d\Delta\omega C(\Delta\omega) \Delta\omega \sin\left(\Delta\omega \frac{\Delta t}{2}\right) \right)^2}{1 - \left(\int d\Delta\omega C(\Delta\omega) \cos\left(\Delta\omega \frac{\Delta t}{2}\right) \right)^2}. \end{aligned} \quad (\text{D2})$$

In the regime of small separations $\sigma_t \Delta t \ll 1$, in which the wavepackets are mostly overlapping, we can neglect the higher orders in Δt in the Taylor expansion of Eq. (D2), obtaining:

$$F(\Delta t) \simeq \frac{1}{4}\eta \frac{\left(\frac{\Delta t}{2} \right)^2 \left(\int d\Delta\omega C(\Delta\omega) \Delta\omega^2 \right)^2}{\int d\Delta\omega C(\Delta\omega) \Delta\omega^2} = \eta \frac{\sigma_\omega^2}{2} = \eta \frac{1}{8\sigma_t^2}, \quad (\text{D3})$$

which is the same as the FI in Eq. 6 in the main text. So in the case $\sigma_t \Delta t \ll 1$, it is possible to achieve a constant Fisher Information even using two bucket detectors in the place of resolving cameras.

Appendix E: Maximum likelihood estimation

Here we show how to derive the likelihood estimator for the estimation of the parameter Δt . Knowing the probability, $P_\nu(\Delta\omega_i; X_i|\Delta t)$, of a sampling event in our frequency resolved scheme, we can define the likelihood as

$$\mathcal{L} = \prod_i P_\nu(\Delta\omega_i; X_i|\Delta t), \quad (\text{E1})$$

and consequently, using the explicit expression for the probability in Eq. 4, taking the logarithm of the former expression we can write the log-likelihood as

$$\log \mathcal{L} \propto \sum \log \{1 + \alpha(X_i)\nu \cos(\Delta\omega_i \Delta t/2)\}. \quad (\text{E2})$$

Now, to find the best estimator for the parameter Δt , we impose the maximization of the log-likelihood function with respect to the parameter itself, which translates to

$$\frac{\partial \log \mathcal{L}}{\partial \Delta t} = 0 \implies \sum_i \frac{\alpha(X_i)\nu \sin(\Delta\omega_i \Delta t/2)}{1 + \alpha(X_i)\nu \cos(\Delta\omega_i \Delta t/2)} \Delta\omega_i = 0. \quad (\text{E3})$$

The best estimator $\tilde{\Delta t}$ is found numerically solving the equation for Δt , given the set of values $\{\Delta\omega_i, X_i\}$.

Once we have found the value of the estimator, we can assume that its variance for large finite values of N is given approximately by adding a contribution of the order $\sim 1/N^2$ to the lowest order term $1/NF_\nu$, obtaining

$$\text{Var}(\tilde{\Delta t}) \sim \frac{1}{NF_\nu(\Delta t)} + \frac{a}{N^2 F_\nu(\Delta t)} \implies \text{Var}(\tilde{\Delta t}) NF_\nu(\Delta t) = 1 + \frac{a}{N}, \quad (\text{E4})$$

where a is the coefficient that tells us how fast the Cramér-Rao bound is saturated. Using the data obtained by the numerical simulation shown in Fig. 3, we can fit to obtain the value of a . We show the goodness of fit parameters in the Table I in the main text. As we can see the R-square values are all above 0.9. The Summed square of residual is at most of the order of 10^{-3} , which tells us that the model is accurate.